

June 2014

## Using Fine Resolution Orthoimagery and Spatial Interpolation to Rapidly Map Turf Grass in Suburban Massachusetts

Daniel S.M. Runfola  
*The College of William and Mary, dan@danrunfola.com*

Thomas Hamill  
*Clark University*

Robert Gilmore Pontius Jr.  
*Clark University, rpontius@clarku.edu*

John Rogan  
*Clark University, jrogan@clarku.edu*

Nick Giner  
*Clark University*

Albert Decatur  
*The College of William and Mary*  
Follow this and additional works at: <http://dc.uwm.edu/ijger>

 Part of the [Earth Sciences Commons](#), [Environmental Sciences Commons](#), and the [Geography Commons](#)  
*Clark University, sratick@clarku.edu*

### Recommended Citation

Runfola, Daniel S.M.; Hamill, Thomas; Pontius, Robert Gilmore Jr.; Rogan, John; Giner, Nick; Decatur, Albert; and Ratick, Samuel (2014) "Using Fine Resolution Orthoimagery and Spatial Interpolation to Rapidly Map Turf Grass in Suburban Massachusetts," *International Journal of Geospatial and Environmental Research*: Vol. 1: No. 1, Article 4.  
Available at: <http://dc.uwm.edu/ijger/vol1/iss1/4>

---

# Using Fine Resolution Orthoimagery and Spatial Interpolation to Rapidly Map Turf Grass in Suburban Massachusetts

## **Abstract**

This paper explores the use of spatial interpolative methods in conjunction with object based image analysis to estimate turf grass land cover quantity and allocation in Greater Boston, Massachusetts, USA. The goal is to learn how accurately turf grass can be estimated if only a limited portion of the study area is mapped. First, turf grass land cover is mapped at the 0.5 m resolution across the entire Plum Island Ecosystems (PIE) Long Term Ecological Research (LTER) site, a 1143-km<sup>2</sup> area. Second, the turf grass map is aggregated into 120 m cells (N = 84,661). Third, a random sample of these 120 m cells are selected to generate an estimate of the unselected cells using four estimation methods - Inverse Distance Weighting, Kriging, Polygonal Interpolation, and Mean Estimation. The difference between known and estimated values is recorded using 120 m cell and census block group stratifications. This process is repeated 500 times for sample sizes of 2.5%, 5.0%, 7.5% and 10.0% of the study area, for a total of 2000 iterations. The average error statistics are reported by sample size, strata, and estimation method. Inverse distance weighting performed best in terms of total error across all sample sizes. It was found that by mapping only 2.5% of the study area, all four methods outperformed a recently published approach to estimating turf grass in terms of overall error.

## **Keywords**

Turf grass, suburbanization, object-based image analysis, interpolation

## **Acknowledgements**

The United States' National Science Foundation (NSF) supported this work via the following programs: Long Term Ecological Research via grants OCE-0423565 & OCE-1026859 for Plum Island Ecosystems and OCE-0620959 for Georgia Coastal Ecosystems, Coupled Natural Human Systems via grant BCS-0709685, Research Experiences for Undergraduates via grant SES-0849985, and Urban Long Term Research Areas via grant BCS-0948984. NSF supplied additional funding through a supplement grant entitled "Maps and Locals (MALS)" via grant DEB-0620579. Any opinions, findings, conclusions, or recommendation expressed in this paper are those of the authors and do not necessarily reflect those of the funders. Anonymous reviewers supplied constructive feedback that helped to improve this paper.

## 1. INTRODUCTION

### 1.1 RESEARCH QUESTION

Turf grass, including lawns on residential properties and parks, is a critical land cover which has key environmental implications – for example, large lawns can lead to changes in outdoor water use and fertilization, reduce the impact of the urban heat island, and even have ramifications for regional carbon cycles (Gober et al. 2010; Milesi et al. 2005; Polsky et al. 2014; Robbins and Birkenholtz 2003). However, mapping turf grass using traditional remote sensing approaches can be prohibitively resource intensive in terms of both human and monetary capital (Giner et al. 2013; Mathieu et al. 2007; Milesi et al. 2005; Runfola et al. 2013a). In this paper we explore the use of spatial interpolative methods in conjunction with a mapped product produced using object based image analysis (OBIA) to rapidly estimate turf grass land cover in Greater Boston, MA. We also compare our findings to a recently published methodology for the rapid approximation of turf grass, a coarse resolution (1 km) approach used by Milesi et al. (2005; 2009). This research aims to answer the question: “Given a limited level of resources available for mapping, what method most accurately estimates the quantity and allocation of turf grass?”

This question is critical for researchers hoping to examine the impacts of turf grass over large areas. Mathieu et al. (2007) found that, while OBIA-approaches saved time when compared to manual digitization, it could still take up to two months to map a 36 km<sup>2</sup> area using 4 m spatial resolution data. Using Mathieu’s estimates, to map turf grass across the United States land area (9.16 million km<sup>2</sup>) using 4 m data would take over 42,000 years. The infeasibility of this strictly OBIA-based approach necessitates exploring available alternatives. Here, we explore using spatial interpolation in conjunction with limited scope OBIA-based mapping. Spatial interpolative methods have been applied to a wide variety of phenomena, including precipitation (Daly et al. 1994; Goodale et al. 1998), air quality (Briggs et al. 2000; Lipfert and Wyzga 1997), ores (Isaaks and Srivastava 1989), submersed vegetation (Valley et al. 2005), and soil contamination (Cattle and Minasny 2002). However, these methods are rarely employed in conjunction with remotely sensed data, and have not been previously applied to the estimation of turf grass.

### 1.2 LITERATURE REVIEW

Turf grass is broadly characterized by non-native, irrigation-dependent grass species, generally found around single-family houses, sidewalks, parks, golf courses, and other land uses (Milesi et al. 2005). Increases of turf grass land cover in the United States over the past several decades have been associated with suburban sprawl, which is a widespread trend with ecological, economic, and environmental implications (Milesi et al. 2005; Robbins and Birkenholtz 2003).

To better understand the impact of lawns scientists have noted the need to quantify the extent of turf grass (Milesi et al. 2009; Milesi et al. 2005; Robbins and Birkenholtz 2003). However, the heterogeneous nature of the (sub)urban landscape requires fine spatial

resolution imagery to accurately visualize and quantify turf grass (Milesi et al. 2009; Zhou et al. 2008). As Milesi et al. (2009) notes:

“The cost of such [fine spatial resolution] images and the computation requirements of their analysis still make direct mapping of irrigated areas elusive for regional assessments of urban irrigated areas. Even at a local scale, estimates of urban irrigated areas, let alone maps, are hard to find” (p. 218).

In light of this assertion, several studies have estimated the extent of turf grass vegetation in the United States (Vinlove and Torla 1994; Milesi et al. 2005). Vinlove and Torla (1994) produced a nationwide estimate of lawn cover (71,629 km<sup>2</sup>) based on data from 10 states<sup>1</sup> using a relationship derived from parcel-scale measurements conducted by the Federal Housing Administration and the Census Bureau. While they provided one of the first estimates of lawn cover, the method employed by Vinlove and Torla has at least two limitations. The first is scale – the finest scale at which estimates are provided is for U.S. states (i.e., one estimate for all of "Massachusetts" or "Colorado"), limiting the ability of researchers to use this data for finer-scale studies. Second, a lack of measurements of lawns across all U.S. states prevented Vinlove and Torla from fully validating their estimates.

In another study, Milesi et al. (2005) produced an estimate of turf grass coverage using sets of aerial photographs spanning eighty 1x1 km grid cells located across thirteen major metropolitan areas<sup>2</sup>. These images were manually digitized to determine the proportion of both turf grass and impervious surfaces. The relationship between the fraction of impervious surface and turf grass surface ( $R^2 = 0.69$ ) was then used in conjunction with a United States wide impervious fraction estimate to produce the final estimate of turf grass quantity. In a later study, Milesi et al. (2009) updated this approach utilizing two new sources of information on the extent of impervious surfaces (urbanized areas), revising their estimates of turf grass coverage in the U.S. to 111,722 km<sup>2</sup> (when using USGS impervious information) and 161,634 km<sup>2</sup> (when using NOAA impervious information). Additionally, Milesi et al. (2009) compare their remote sensing approach to an approach similar in nature to the one employed by Vinlove and Torla, producing estimates ranging from 72,640 km<sup>2</sup> to 145,641 km<sup>2</sup> of turf grass. The range in these estimates highlights the discrepancy between the resolvability of turf grass in imagery and the objectives of previous studies that seek to quantify turf grass at coarse spatial resolutions (e.g., 1km) (Milesi et al. 2009; Strahler et al. 1986).

### **1.3 STUDY REGION**

This study focuses on a group of 26 suburban towns to the north of the city of Boston (Figure 1): the Plum Island Ecosystems (PIE). PIE covers approximately 1150 km<sup>2</sup> in

---

<sup>1</sup> Illinois (1977), Kentucky (1989), Maryland (1986), Michigan (1988), Montana (1983), New Jersey (1983), North Carolina (1986), Ohio (1989), Oklahoma (1987), and Pennsylvania (1989). Vinlove and Torla, 1995 (pg. 88).

<sup>2</sup> Atlanta, Boston, Chicago, Denver, Houston, Las Vegas, Miami, Minneapolis, New York, Phoenix, Portland, Sacramento, Seattle

northeastern Massachusetts (LTER 2010), with 21% of the area utilized for residential land (MassGIS 2011). This region has experienced tremendous growth over the recent past, making it ideally suited for mapping the effects of U.S. suburbanization. Population in metropolitan Boston has decreased over the past three decades, as its suburbs have experienced substantial development and increases in population (Tu et al. 2007; US Census 2009). The number of new housing permits allotted in the region between 2000 and 2006 exceeded 55,000 (MAPC 2010). Further, the average housing lot size doubled in the Boston region between 1970 and 2000, suggesting a possible growth in lawn size (MAPC 2010).

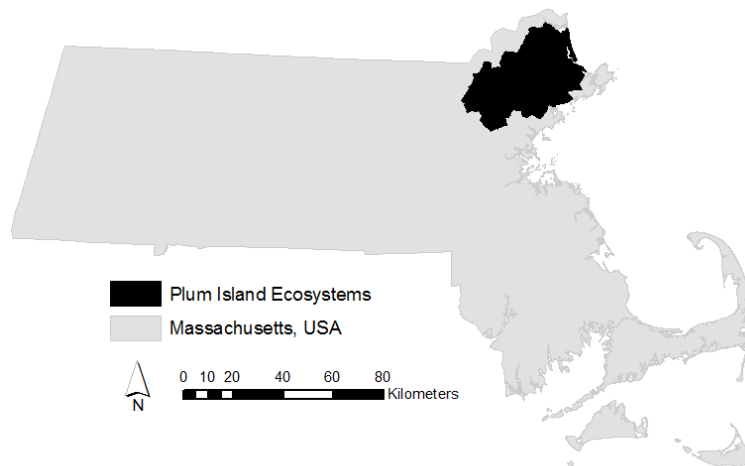


Figure 1. Plum Island Ecosystem study region within the state of Massachusetts.

## 2. METHODS

### 2.1 DATA

Remotely sensed data were derived from digital 8-bit, four-band (blue, green, red and near-infrared) orthoimagery captured between April 9 and April 17, 2005 (leaf-off) with a 45 cm spatial resolution (MassGIS 2011). These data were geometrically corrected and resampled to a 50 cm resolution using bilinear interpolation (MassGIS 2011). Ancillary data included year 2003 assessor's parcels, a wetlands layer, and both a 1 m impervious surfaces layer and 2005 land use layer. Census boundaries from the year 2000 were acquired from the US Census Bureau (US Census 2010). This data was used to facilitate the object-based image analysis mapping of turf grass across the study area at the 0.5 m resolution. As summarized in tables 1 and 2, accuracy assessment indicated 94% accuracy when reclassified to only "turf grass" and "other" (Polsky et al., 2012; Runfola et al., 2013b). For further information on the calculation of population-adjusted cross-tabulation matrices for accuracy assessment, see Pontius and Millones (2011).

Table 1. The population-adjusted proportional crosstabulation for the Plum Island Ecosystems 0.5 meter mapping product. The overall proportionally adjusted percent correct is 79.64%.

		<b>Photo Interpreter</b>							
		<b>Bare Soil</b>	<b>Conif. Trees</b>	<b>Decid. Trees</b>	<b>Turf Grass</b>	<b>Imperv.</b>	<b>Water</b>	<b>Wet-land</b>	<b>Map Total</b>
<b>Map</b>	<b>Bare Soil</b>	2.32	0.01	0.34	0.65	0.33	0	0.09	3.74
	<b>Coniferous</b>	0.04	9.77	2.45	0.37	0.07	0.06	0.07	12.83
	<b>Deciduous</b>	0.55	1.59	29.62	1.73	0.27	0.28	0.63	34.68
	<b>Turf Grass</b>	1.29	0.23	0.88	9.87	0.41	0.04	0.02	12.73
	<b>Impervious</b>	0.49	0.06	0.3	0.17	13.61	0.02	0	14.64
	<b>Water</b>	0.02	0.02	0.09	0.01	0	2.65	0.18	2.97
	<b>Wetlands</b>	0.45	0.62	4.67	0.08	0.04	0.74	11.79	18.4
<b>Photo Total</b>		5.16	12.3	38.35	12.88	14.73	3.79	12.78	100

Table 2. The population-adjusted proportional crosstabulation for the Plum Island Ecosystems 0.5 meter mapping product, adjusted to include only turf grass and other categories. The overall proportionally adjusted percent correct is 94.11%.

		<b>Photo Interpreter</b>		
		<b>Turf Grass</b>	<b>Other</b>	<b>Map Total</b>
<b>Map</b>	<b>Turf Grass</b>	9.87	2.87	12.74
	<b>Other</b>	3.01	84.24	87.25
	<b>Photo Total</b>	12.88	87.11	100

## 2.2 METHODS OVERVIEW

A three-step approach is taken to identify the most accurate method for the prediction of turf grass land cover:

- 1) The entire PIE region is mapped at 0.5 m resolution using Object Based Image Analysis (OBIA) to produce a map of turf grassland cover.
- 2) These data are aggregated to 120 m cells (see Figure 2), and a 2.5% sample of these 120 m cells in the PIE region is randomly selected and used to generate an interpolated estimate for each of the unsampled 120 m cells using four approaches. This is repeated five hundred times, each time with a different random sample, and results are recorded for each iteration.
- 3) This process is repeated for sample sizes of 5.0%, 7.5%, and 10.0% of the study area to assess the relationship between increased sample size and accuracy.

## 2.3 TESTING PREDICTIVE METHODS IN PIE

Five methods, four interpolative (inverse distance weighting, kriging, polygonal, and a mean method), and one extrapolative (the regression approach proposed in Milesi 2005; 2009) are compared to determine which provides the highest accuracy for the estimation of turf grassland cover at the 120 m cell and census block group stratification, as well as at the global scale (i.e. the full study area). First our 0.5 meter resolution mapping product is aggregated to 120 m cells across the study area, so that the proportion of turf grass in each 120 m area is known. Second, 2.5% ( $n=2,030$  120 m cells) of these cells are randomly selected. These selected cells are then used to predict the proportion of turf grass in unselected cells using each of the estimation procedures. This process is repeated 500 times following a Monte Carlo random selection procedure, and the difference between the predicted and mapped turf grass amount is recorded for all methods using two stratifications, 120 m cells and census block groups. These stratifications were chosen on the basis of their usefulness in aligned research projects: 120 m cells provide a high degree of information on spatial location useful for household-scale studies, while census block groups give access to socio-demographic and economic data from the US Census.

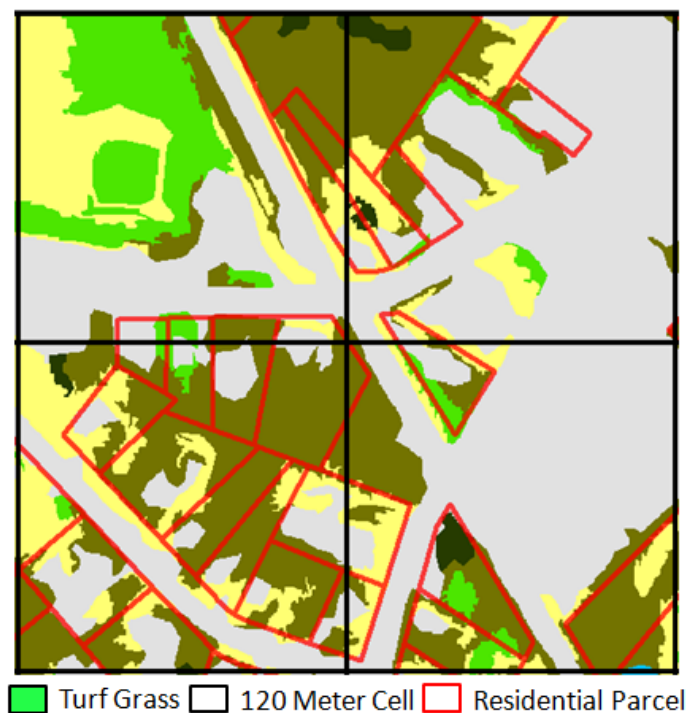


Figure 2. An example of the aggregation procedure followed for each 120-meter cell. All turf grass within a 120 meter cell was summed and attributed to the cell within which it fell. Other classes that appear in this map include coniferous trees (dark green), deciduous trees (dark brown), bare soil (yellow) and impervious surface (grey).

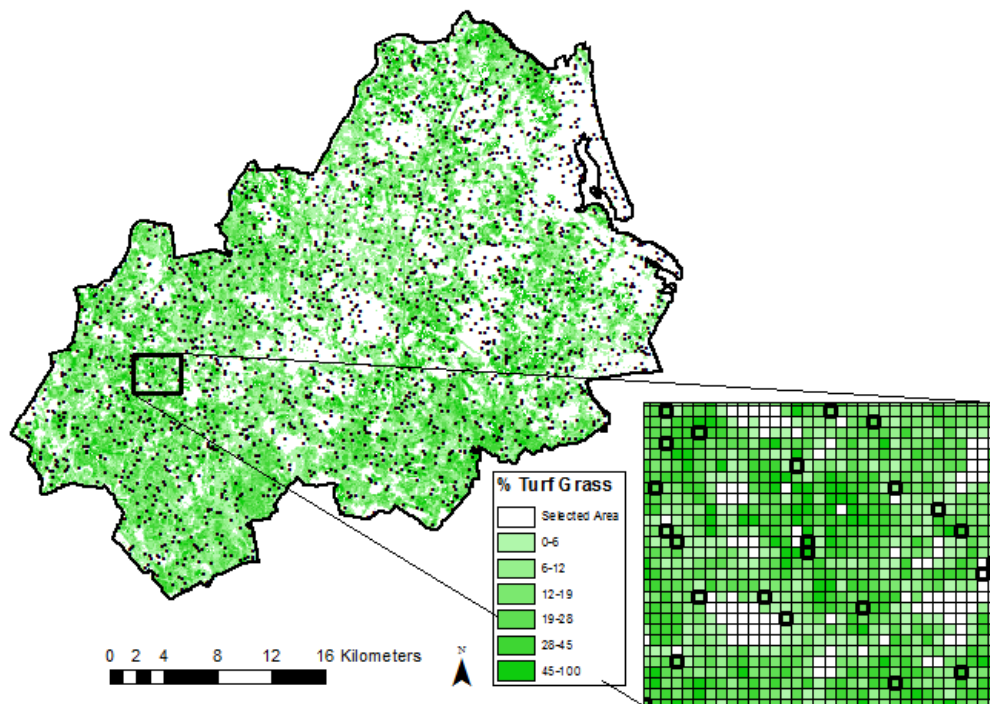


Figure 3. Turf grass vegetation reference map is on the left in which black points represent a sample ( $n=2.5\%$ ). A zoomed-in sample of the map is on the right, in which each 120 meter cell can be seen, as well as the selected cells in bold outline.

This process is repeated to assess the relationship between increased sample size and accuracy. In addition to a sample size of 2.5% ( $n=2,030$  120 m cells), 5% ( $n=4,061$ ), 7.5% ( $n=6,091$ ) and 10% ( $n=8,122$ ) of the study area were also tested for a total of 2000 Monte Carlo simulations (500 per sample size). Figure 3 shows one sample iteration in which 2,030 (2.5%) of all 81,215 120 m cells are outlined in black, representing a single random sample.

Aggregation to the census block group stratification is performed by tallying the total square meters of turf grass in each 120 m cell (mapped or estimated) that is contained within a given census block group. In cases where a single cell overlapped multiple blocks, the amount of turf grass was split according to the areal proportion of the cell overlapping each census block group following Goodchild (1993; 1980). Global turf grass quantity was also calculated by summing the total estimated turf grass in all 120 m cells.

The fifth method tested comes from Milesi (2005; 2009). A single map of turf grass land cover was created using the regression relationship found in Milesi (2005; 2009). This map was compared to our high resolution mapping product following the same procedure as each interpolation method.

### 2.3.1 MILESI AND THE MEAN METHOD: ASPATIAL ESTIMATION

As a comparison to past literature, we employ the relationship for fractional turf grass area developed by Milesi et al. (2005; 2009) following the linear regression method described in the literature review:

$$y = 79.53 - 0.83 * I \quad (1)$$

where  $y$  is the percent of turf grass cover and  $I$  is the percent of impervious surface land cover. Impervious data with a spatial resolution of 1 km for the entire study area is derived from the USGS NLCD Impervious Surface dataset used in Milesi (2009). Within each 1 km cell, the amount of turf grass is calculated following equation 1, and each census block group is assigned a value according to the cell(s) it overlapped following the Goodchild (1993; 1980) approach described earlier.

The second aspatial method tested here is also, by design, the simplest: the mean method. The mean method is calculated by determining the mean area of turf grass land cover of all sampled 120 m cells, and applying this mean value to the remaining (unsampled) cells in the area. This method serves as a baseline to compare against the accuracy of the more complex spatial methods.

### 2.3.2 POLYGONAL INTERPOLATION

The first of the spatial predictive methods tested, polygonal interpolation, assigns the value of the closest sample cell to any unsampled cells (Isaaks and Srivastava 1989). This approach is closely related to the inverse distance weighting approach, but requires a great deal less computational time to calculate. In application, the centroid (calculated by averaging the x,y coordinates within the 120 m cell) is used to determine the distances between any two cells (c.f. Cai et al. 2006).

### 2.3.3 INVERSE DISTANCE WEIGHTING

Inverse Distance Weighting (IDW) estimates values on the basis of a weighted linear combination in which weights are assigned according to the distance from an unknown point to a known point (Shepard 1968; Isaaks and Srivastava 1989). A power parameter ( $p$ ) determines the rate at which influence decreases with distance (Shepard 1968). For this analysis, a power parameter of 2 is used due to its common use (ESRI, 2007).

### 2.3.4 ORDINARY KRIGING

In ordinary kriging, non-sampled 120 m cells are assigned a value according to a weighted linear combination (WLC) of all sampled point values in which the weights are derived on the basis of a statistical covariance function that is estimated from the sampled cells (Isaaks and Srivastava 1989). This is done by examining how similar sampled cell values are a given distance apart (the lag distance). As the lag is varied from smaller to larger distances, the resulting covariance relationship is obtained. In practice geostatisticians estimate a related measure, the variogram, to calculate the interpolation weights.

## 2.4 METHOD COMPARISON

The results of each method are recorded for each of the random samples drawn, and the difference between the predicted turf grass area and mapped turf grass area are summarized in terms of mean absolute error, separated into three components: quantity error, allocation error at the census block group stratification, and allocation error at the 120 m cell stratification (Pontius and Millones, 2011; Pontius et al., 2008). Quantity error can be interpreted as the difference in the amount of turf grass area in the entire spatial extent. It is calculated following:

$$E_q = \left| \sum_{b=1}^B Z_b - Y_b \right| \quad (2)$$

where  $E_q$  is the quantity error,  $B$  is the total number of census block groups,  $b$  is a unique identifier for each census block group,  $Z_b$  is the mapped square meters of turf grass within census block group  $b$ , and  $Y_b$  is the predicted square meters of turf grass in census block group  $b$ . Total quantity error is identical regardless of the stratification chosen for calculation (e.g., 120m cells vs. census block groups).

Allocation error is calculated using two levels of stratification: the census block groups and the 120 m cells following the equations in Pontius et al. (2008). Allocation measures how much less than perfect the model assigns turf grass spatially across the landscape, which is a task that becomes more challenging as the map units used for spatial stratification become smaller. For the census block group stratum it is calculated following equations 3 - 4:

$$E_g = \sum_{b=1}^B |Z_b - Y_b| \quad (3)$$

$$E_a = E_g - E_q \quad (4)$$

where  $E_g$  is total error at the level of the census block group stratification and  $E_a$  is allocation error at the level of the census block group stratification. Equations 5-6 provide the approach to calculating additional allocation error introduced by examining estimates using 120 m cells for stratification:

$$E_f = \sum_{h=1}^H |M_h - P_h| \quad (5)$$

$$E_k = E_f - E_q - E_a \quad (6)$$

where  $E_f$  is total error in the 120 m cell stratification,  $E_k$  is additional allocation error introduced when moving from the census block group stratification to the 120 m cell stratification,  $H$  is the total number of 120 m cells,  $h$  is a unique identifier for each 120 m cell,  $M_h$  is the mapped square meters of turf grass within 120 m cell  $h$ , and  $P_h$  is the predicted square meters of turf grass in 120 m cell  $h$ . The average value is reported by method for all iterations for quantity error ( $E_q$ ) and allocation error at both the census block group ( $E_a$ ) and 120 m cell ( $E_k$ ) stratification. These three components sum to total error at the 120 m stratification ( $E_f$ ). Figure 4 contains an example output of this type of

analysis. The stacked bar represents the three errors examined: quantity, allocation in the census block group stratification, and allocation in the 120 m cell stratification. The black portion of the bar is quantity error. The white portion of the bar is the allocation error in the census block group stratification, while the height of the white and black portions together are total error in the census block group stratification. The grey portion of the bar represents additional allocation error introduced when using the 120 m cell stratification. The height of the white and grey bars together represents total allocation error using the 120 m stratification. The total height of the bar represents total error when using the 120 m stratification.

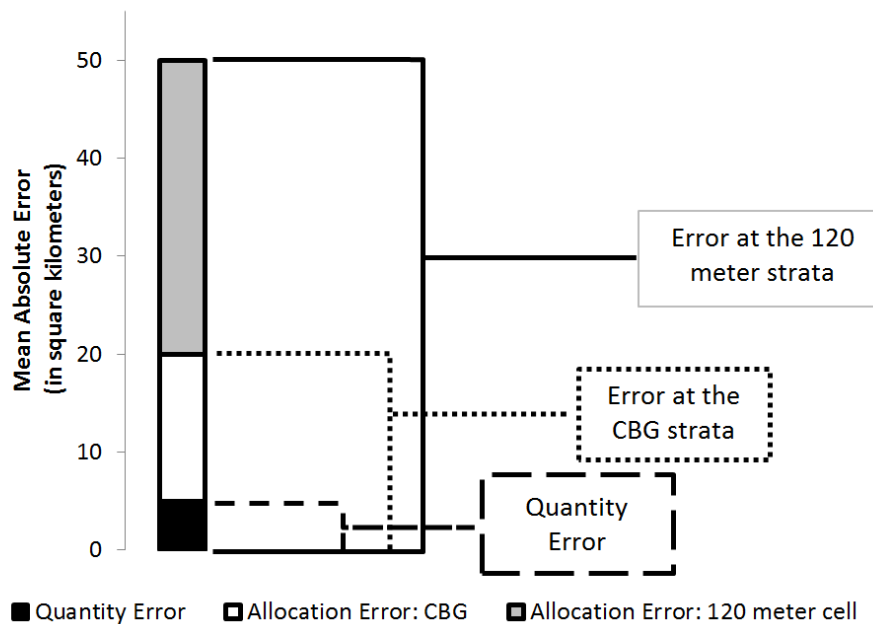


Figure 4. An example graphical output of quantity error, allocation error at the census block group stratification, and allocation error at the 120 meter cell stratification.

### 3. RESULTS

#### 3.1 MAPPING PIE

Figure 2 shows an example of four of the ~80,000 120 m cells, and the underlying 0.5 m mapping data resulting from the mapping effort, and tables 1 and 2 show the results from the validation. Across the entire study area, the 120 m cells range from containing zero m<sup>2</sup> (no turf grass) to 14,400 m<sup>2</sup> (fully turf grass). Within census block groups, coverage ranges from a minimum of 2.1% to a maximum of 38.6% turf grass land cover (square meters of turf grass range from .01 km<sup>2</sup> to 3.31 km<sup>2</sup>). The total turf grass in the region is 145 km<sup>2</sup>, i.e. 12.7% of the study area. Census block groups located closer to town centers

tended to have greater proportions of turf grass land cover, although they generally had less total area of turf grass due to their smaller sizes.

### **3.2 METHOD TESTS IN THE PLUM ISLAND ECOSYSTEMS**

Figure 5 shows a single random sample ( $n=2.5\%$ ; 2,030 120 m cells) and associated prediction for each method as a representative example of each interpolation's output. Figure 6 has four charts, each with the error on the y axis and the percentage of the PIE study area sampled on the x axis to provide an indicator of the accuracy of each method by sample size. The stacked bars in this figure are representative of the three measurements of error: quantity error, allocation error using the census block group stratification, and allocation error when using the 120 meter cell stratification.

In terms of quantity error, the inverse distance weighting approach works best when the smallest sample size is taken (2.5%), but the polygonal method performs best for all larger sample sizes with an average quantity error of 2.29 square kilometers. Inverse distance weighting method has the smallest allocation error when using both the census block group and 120 m cell stratifications, regardless of sample size. It had an average of 21.19 km<sup>2</sup> of allocation error across all sample sizes and CBGs, and 83.0 km<sup>2</sup> across all 120 m cells. The inverse distance weighting approach also had the least overall error across all sample sizes. Using the census block group stratification, IDW outperformed the worst performing model, the mean model, by between 21 km<sup>2</sup> (2.5% of the study area sampled) and 35 km<sup>2</sup> (10%). Using the 120 m cell stratification, IDW outperformed the mean model by between 25 km<sup>2</sup> (2.5%) and 48 km<sup>2</sup> (10%).

The Milesi (2005; 2009) approach over predicted the true turf grass quantity by 40.9 km<sup>2</sup>. For the census block group stratification, the Milesi approach had 49.2 km<sup>2</sup> of allocation error, for a total of 91.1 km<sup>2</sup> of error. For the 120 m cell stratification, the Milesi approach had 110.7 km<sup>2</sup> of additional allocation error, for a total of 201.8 km<sup>2</sup> of error.

The average error across all sample sizes for each method is shown in figure 7. Inverse distance weighting performed best in terms of total error, closely followed by the kriging and polygonal approaches. In terms of quantity error the inverse distance method also performs best on average, but the overall lowest quantity error was found for the polygonal approach with a sample size of 10%. For census block groups, the IDW and kriging methods performed similarly in terms of allocation error, with an average of 21.2 (IDW) and 23.0 (kriging) km<sup>2</sup> of allocation error.

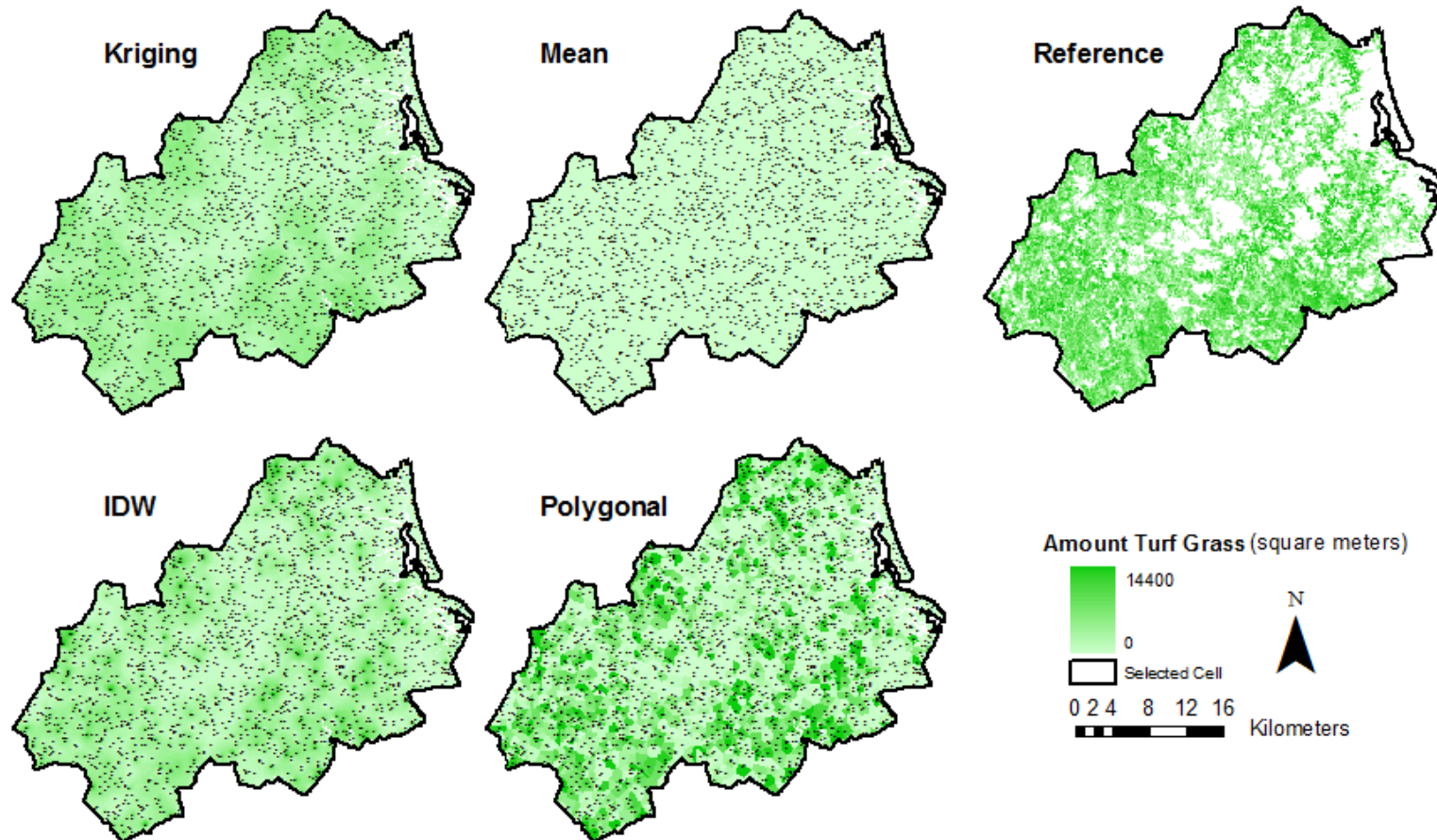


Figure 5. Predictive maps for all four predictive approaches. Black points represent sampled 120 meter cells used for interpolation.

The standard deviation of quantity error was calculated for the mean, polygonal, IDW, and kriging approaches, and can be seen in figure 8. The mean model had the largest average standard deviation across all sample sizes, 2.9 km<sup>2</sup>. The remaining methods performed very similarly, with the Polygonal method, IDW, and kriging having average standard deviations of 1.74, 1.71, and 1.86 km<sup>2</sup> respectively.

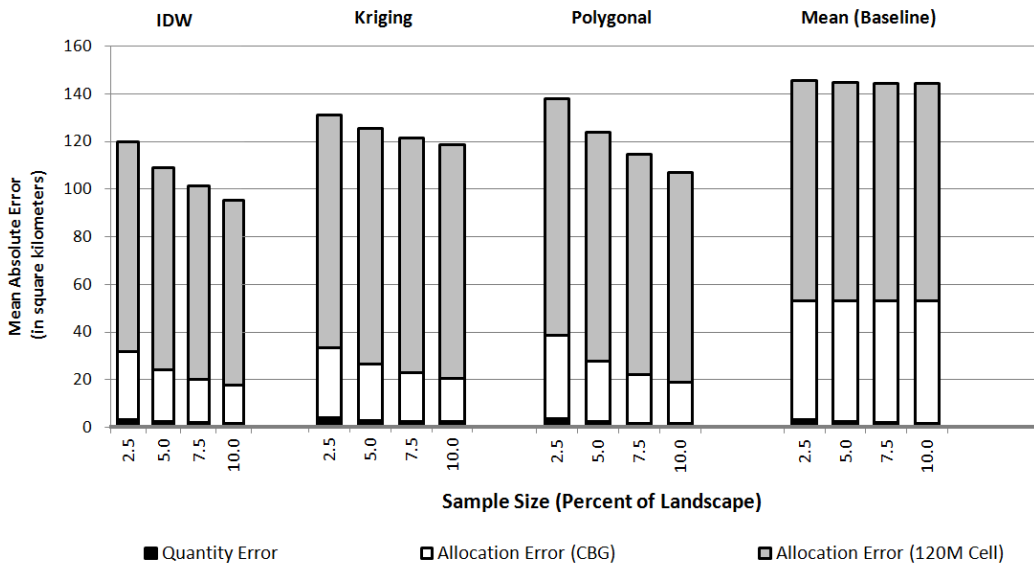


Figure 6. Figures illustrating the relationship among errors, sample sizes, and approaches. The true quantity of turf grass on the landscape is 145 square kilometers.

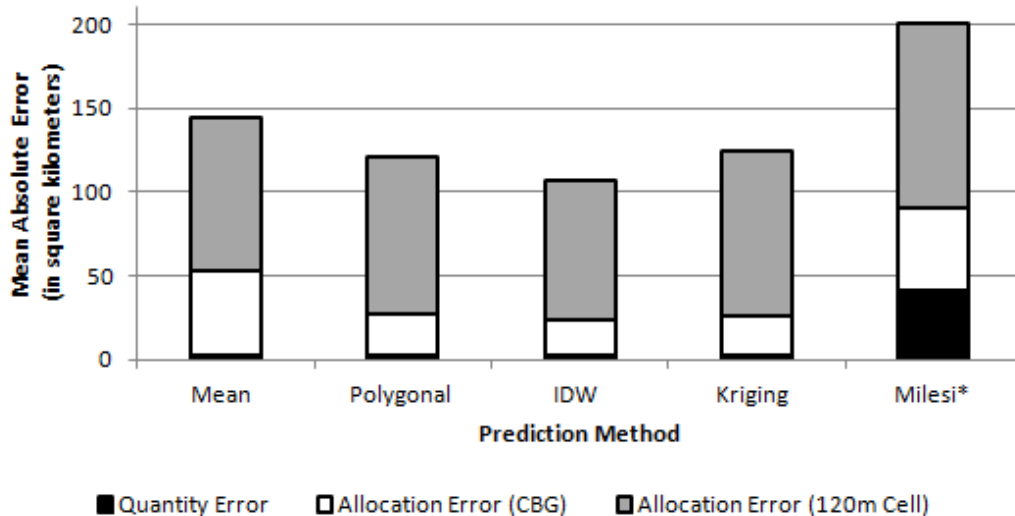


Figure 7. The average error across all sample sizes for each method. \*The Milesi method is based on a single population dataset.

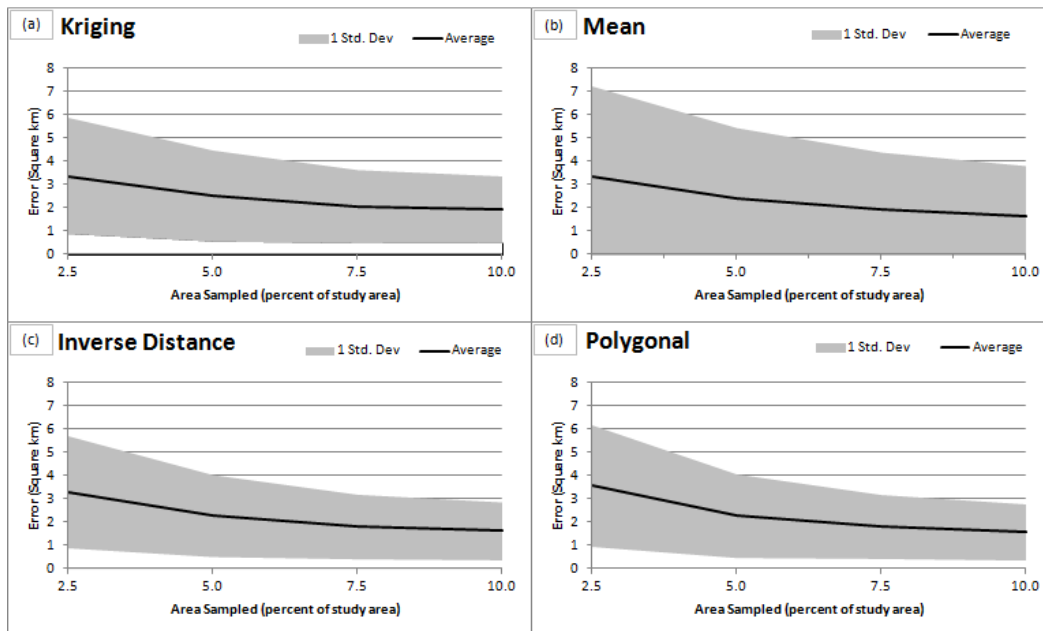


Figure 8. The average quantity error and standard deviation of quantity error across all sample sizes for each method.

The directionality of error was not always the same, and varied across methods. The mean method overestimated 51% of the time – nearly a perfect split between over and under-estimation due to the random sampling approach. The Inverse Distance Weighting, kriging, and Polygonal methods all performed similarly, overestimating 68%, 68%, and 62% of the time, respectively. For each of these methods, as more samples were taken they tended to overestimate more often.

#### 4. DISCUSSION

Scale played a large role in determining the accuracy of all methods. Across the entire study area all methods provided strong estimates of the observed, total quantity of turf grass (represented by the black bars in figure 6). Allocating this quantity to the census block group scale introduced a moderate amount of error (the white portion of the bars in figure 6), and allocating to the 120 m cell scale introduced a large amount of error (the grey portion of the bars in figure 6). This suggests that spatial interpolative methods for examining turf grass will work best across coarser units of analysis (i.e., census block group and coarser), and moving to finer scales can only be done at the cost of accuracy.

In this study, inverse distance weighting (IDW) was the best performing method for every sample size in terms of census block allocation, 120 m cell allocation and total error. In the case of PIE, this is likely due to IDW's integration of spatial information, which the mean method does not do, and the polygonal method only does to a limited degree. IDW's performance when compared to kriging is likely attributable to how each

equation incorporates spatial dependence. IDW defines spatial dependence as a single distance-decay value ( $p$  in equation 3) irrespective of the sample taken, whereas kriging re-calibrates spatial dependence on the basis of the variogram for any given sample. A polynomial best-fit line is used to estimate the variogram in our Monte Carlo approach, therefore in some cases over-fitting may lead to poor results if compared to a manually calibrated relationship. Additionally, in cases where the random sample is not representative of the landscape, the variogram will also not be representative of the landscape, potentially leading to a more erroneous prediction. In these cases the decay function defined by the researcher in IDW ( $p$ ) may be closer to the mapped reality than the variogram calculated during the kriging calibration process. In an environment where each variogram is manually calculated, kriging may show stronger results.

For the sample size of 10% of the study area, the polygonal method produced the most accurate estimations of the quantity of turf grass. This can be attributed to the high degree of similarity between neighboring census block groups turf grass amounts in the PIE study region. This was verified by calculating a Moran's I score, which provides a single value indicating the spatial autocorrelation of the phenomenon of interest. Values approaching +1 indicate neighboring locations are more similar, while those approaching -1 indicate neighboring locations are dissimilar. In this case, the Moran's I for the closest neighbor(s) (those that share a border) was 0.61, indicating a high degree of similarity between neighboring 120 m cells. Because the polygonal approach always takes the closest sampled cell value for any unsampled cell, study areas with very high first-order spatial autocorrelation will see strong results from this approach.

The mean model performed similarly to the polygonal, IDW, and kriging methods in terms of quantity error, but performed much worse in terms of allocation error. This is unsurprising, as the mean approach does not incorporate any spatial information in its allocation of turf grass. Because spatial autocorrelation exists in this study area, those methods that do incorporate spatial information were better able to estimate the allocation of turf grass across the study area.

For all four methods, the largest gains in accuracy per area sampled are found when the sample size increases from 2.5% to 5.0% of the landscape. The increases from 5.0% to 7.5% and 7.5% to 10.0% were subject to diminishing returns in terms of overall gains in accuracy. The majority of the gains in accuracy were due to improved allocation of turf grass, leading to an increasing disparity between the mean approach (which – by design - did not see a benefit to allocation as the sample size increased) and the interpolative methods.

All three methods which relied on spatial information, IDW, kriging, and Polygonal, overestimated the total turf grass in the study area more than 60% of the time. In the case of kriging, this bias is partially explained by a limitation on the lower bound of predictions (that is, no cell was allowed to be predicted with a negative amount of turf grass). In all three interpolative models, this bias is also attributable to the likelihood a cell which has a mapped value of zero will also have a predicted value of zero. If a single value greater than zero falls within the search radius of an unknown point, then the value of the cell to be predicted will also be greater than zero. Larger search radii (or otherwise including more neighboring points) could potentially exacerbate this issue.

The Milesi (2005; 2009) remote sensing approach over-predicted the true quantity of turf grass by 49.2 km<sup>2</sup>. In terms of census block group allocation error it outperformed the mean method for all sample sizes, but has a larger 120 m cell allocation error, quantity error, and overall error than all other approaches. In terms of quantity error Milesi is always the worst performing model, where even at the smallest sample size it has over ten times the error of the next-worst performing model (Polygonal). This is not surprising, as the Milesi analysis was not designed to allocate turf grass to spatial units smaller than 1 km and was calibrated for nationwide estimations.

Many other approaches could potentially mitigate some of the limitations of this method. For example, stratified sampling would likely improve both the accuracy and efficiency of hybrid mapping and interpolative approaches. Further, the scale at which underlying data is produced could have important implications for resource investment – research could examine if 0.5 meter mapping is sufficient or finer than necessary for the varied applications of information on lawn landscapes. Additionally, further research on the applicability of these findings to other research domains should be conducted before nationwide hybrid mapping projects are undertaken.

## 5. CONCLUSIONS

This paper explores the use of spatial interpolative methods in conjunction with object based image analysis to estimate turf grass land cover over a large spatial extent. It seeks to answer the question: “Given a limited level of resources available for mapping, what method most accurately estimates the quantity and allocation of turf grass?” We evaluated ordinary kriging, inverse distance weighting, polygonal, and a sample mean method in conjunction with a 0.5 m object-based image analysis classification in a Monte Carlo framework. Additionally, we evaluated the remote sensing based extrapolative approach used in Milesi et al. (2005; 2009). In terms of estimating the overall quantity of turf grass land cover, the IDW method performs best for when 2.5 to 7.5% of the landscape is mapped, and polygonal interpolation performs best when 10% of the landscape is mapped. IDW performs best in terms of the allocation of turf grass to 120 m cells and census block groups within the study area. In terms of overall error, inverse distance weighting performs best regardless of sample size.

We found that a previous, nation-wide estimate of turf grass published in Milesi et al. (2005; 2009) overestimated the quantity of turf grass by 49.2 square kilometers in the PIE study region. While this is a larger overall error than all predictive methods and sample sizes tested in this paper, the nation-wide scope and relatively low resource need to produce the estimate for very large areas suggests that refining coarse-resolution estimation techniques could be a fruitful research avenue. This would be particularly helpful in regions where fine resolution imagery is not available.

Given a lack of resources with which to conduct fine resolution mapping, the method proposed by Milesi (2005; 2009) provides a strong alternative to the more accurate, but more resource intensive, hybrid object-based image analysis and spatial interpolative approaches. However, if even small areas of the landscape can be mapped (~2.5%) at a

fine resolution, the use of spatial interpolative methods can produce more accurate estimates of the total quantity and allocation of turf grass.

## REFERENCES

- Briggs, D.J., de Hoogh, C., Gulliver, J., Wills, J., Elliott, P., Kingham, S. and Smallbone, K. (2000). A regression-based method for mapping traffic-related air pollution: application and testing in four contrasting urban environments. *The Science of the Total Environment*, 253, 151-167.
- Cattle, J.A.M.B. and Minasny, A.B. (2002). Kriging method evaluation for assessing the spatial distribution of urban soil lead contamination. *Journal of Environmental Quality*, 31, 1576.
- Daly, C., Neilson, R.P. and Phillips, D.L. (1994). A statistical-topographic model for mapping climatological precipitation over mountainous terrain. *Journal of Applied Meteorology*, 33, 140-158.
- ESRI (2007). Implementing Inverse Distance Weighted (IDW).
- Giner, N.M., Polsky, C., Pontius, R.G.J. and Runfola, D.M. (2013). Understanding the social determinants of lawn landscapes: A fine-resolution spatial statistical analysis in suburban Boston, Massachusetts, USA. *Landscape and Urban Planning*, 111, 25-33.
- Gober, P., Brazel, A., Quay, R., Myint, S., Grossman-Clarke, S., Miller, A. and Rossi, S. (2010). Using Watered Landscapes to Manipulate Urban Heat Island Effects: How Much Water Will It Take to Cool Phoenix? *Journal of the American Planning Association*, 76, 109-121.
- Goodale, C.L., Aber, J.D. and Ollinger, S.V. (1998). Mapping monthly precipitation, temperature, and solar radiation for Ireland with polynomial regression and a digital elevation model. *Climate Research*, 10, 35-49.
- Goodchild, M.F., Anselin, L. and Deichmann, U. (1993). A framework for the areal interpolation of socioeconomic data. *Environment and Planning A*, 25, 383-397.
- Goodchild, M.F. and Lam, N.S. (1980). Areal interpolation: a variant of the traditional spatial problem. *Geo-Processing*, 1, 297-312.
- Isaaks, E.H. and Srivastava, R.M. (1989). *An Introduction to Applied Geostatistics* (New York, Oxford University).
- Lipfert, F.W. and Wyzga, R.E. (1997). Air pollution and mortality: the implications of uncertainties in regression modeling and exposure measurement. *Journal of the Air & Waste Management Association*, 47, 517.
- LTER (2010). US Long Term Ecological Research Network.
- MAPC (2010). Metropolitan Area Planning Council (Boston).
- MassGIS (2011). Office of Geographic and Environmental Information (Commonwealth of Massachusetts, Executive Office of Energy and Environmental Affairs).
- Mathieu, R., Freeman, C. and Aryal, J. (2007). Mapping private gardens in urban areas using object-oriented techniques and very high-resolution satellite imagery. *Landscape and Urban Planning*, 81, 179-192.

- Milesi, C., Elvidge, C. and Nemani, R. (2009). Assessing the Extent of Urban Irrigated Areas in the United States. *Remote Sensing of Global Croplands for Food Security*, 217.
- Milesi, C., Running, S.W., Elvidge, C.D., Dietz, J.B., Tuttle, B.T. and Nemani, R.R. (2005). Mapping and Modeling the Biogeochemical Cycling of Turf Grasses in the United States. *Environmental Management*, 36, 426-438.
- Polsky, C., Grove, J.M., Knudson, C., Groffman, P.M., Bettez, N., Cavender-Bares, J., Hall, S.J., Heffernan, J.B., Hobbie, S.E. and Larson, K.L. (2014). Assessing the homogenization of urban land management with an application to US residential lawn care. *Proceedings of the National Academy of Sciences*, 111, 4432-4437.
- Polsky, C., Pontius Jr, R.G., Decatur, A., Giner, N., Rahul, R. and Runfola, D.M. (2012). Mapping Lawns Using an Object-Oriented Methodology with High-Resolution Four-Band Aerial Photography: The Twenty-Six Towns of the Ipswich and Parker River Watersheds, Massachusetts. In George Perkins Marsh Working Paper (Worcester, MA, Clark University).
- Pontius, R., and Millones, M. (2011). Death to Kappa: Birth of Quantity Disagreement and Allocation Disagreement for Accuracy Assessment. *International Journal of Remote Sensing*, 32, 4407-4429.
- Pontius, R., Thontteh, O. and Chen, H. (2008). Components of information for multiple resolution comparison between maps that share a real variable. *Environmental and Ecological Statistics*, 15, 111-142.
- Robbins, P. and Birkenholtz, T. (2003). Turfgrass revolution: measuring the expansion of the American lawn. *Land Use Policy*, 20, 181-194.
- Runfola, D.M., Polsky, C., Giner, N.M., Pontius Jr., R.G. and Nicolson, C. (2013a). Future Suburban Development and the Environmental Implications of Lawns: A Case Study in New England, USA. In *Modeling of Land-Use and Ecological Dynamics*, D. Czamanski, I. Benenson, and D. Malkinson, eds. (New York, Springer Berlin Heidelberg), pp. 119-141.
- Runfola, D.M., Polsky, C., Nicolson, C., Giner, N.M., Pontius, R.G.J., Krahe, J. and Decatur, A. (2013b). A Growing Concern?: Examining the influence of lawn size on residential water use in suburban Boston, MA, USA. *Landscape and Urban Planning*, 119, 112-123.
- Shepard, D. (1968). A two-dimensional interpolation function for irregularly-spaced data. *Proceedings of the 1968 23<sup>rd</sup> ACM national conference*.
- Strahler, A., Woodcock, C. and Smith, J. (1986). On the nature of models in remote sensing. *Remote Sensing of Environment*, 20, 121-139.
- Valley, R., Drake, M. and Anderson, C. (2005). Evaluation of alternative interpolation techniques for the mapping of remotely-sensed submersed vegetation abundance. *Aquatic botany*, 81, 13-25.
- Vinlove, F. and Torla, R. (1994). Comparative estimations of US home lawn area. *Journal of Turfgrass Management*, 1, 83-97.
- Zhou, W., Troy, A. and Grove, M. (2008). Object-based land cover classification and change analysis in the Baltimore metropolitan area using multitemporal high resolution remote sensing data. *Sensors*, 8, 1613-1636.